

A study of the continuum and iron *K* line emission from low-mass X-ray binaries

N. E. White^{1,2}, A. Peacock³, G. Hasinger⁴, K. O. Mason⁵, G. Manzo⁶, B. G. Taylor³, and G. Branduardi-Raymont⁵

¹*EXOSAT Observatory, ESOC, Robert Bosch Str. 5, Darmstadt, W. Germany*

²*Affiliated to Astrophysics Division, Space Science Dept. of ESA*

³*ESA Space Science Department, ESTEC, Noordwijk, The Netherlands*

⁴*Max-Planck Institut für Physik und Astrophysik, Garching, W. Germany*

⁵*Mullard Space Science Laboratory, Holmbury St Mary, Surrey RH5 6NT*

⁶*Istituto di Fisica dell'Universita, Palermo, Italy*

Accepted 1985 August 2. Received 1985 August 2; in original form 1985 July 9

Summary. The spectral properties of a sample of six low-mass X-ray binaries are studied using data obtained with the Gas Scintillation Proportional Counter (GSPC) on *EXOSAT*. The various continuum models proposed for these sources are investigated. Only two-component models provide an acceptable fit to the data. Two possible model combinations were found: in both cases one component was a blackbody with the other either a thermal bremsstrahlung or an unsaturated Comptonized spectrum of low-energy photons on high-energy electrons. The characteristic flaring of these sources is caused by increases in the luminosity of the blackbody component. The thermal bremsstrahlung plus blackbody model was ruled out on the grounds that the derived emission measure infers a dimension for the emission region greater than 10^8 cm. The Compton plus blackbody model can be interpreted in terms of disc accretion on to a neutron star with a low magnetic field. The Comptonized component is identified as coming from the inner disc region, while the blackbody is from the heated surface of a neutron star. An iron *K* emission line centred between 6.4 and 6.8 keV was detected in five out of the six sources with equivalent widths of 70–130 eV and a full-width half-maximum of 1 keV. These results are similar to those of Sco X-1 obtained by the *EXOSAT* GSPC (White, Peacock & Taylor).

1 Introduction

The spectral properties of the luminous X-ray sources that are thought to contain accreting neutron stars can be broadly classified according to whether or not the source is a coherent X-ray

pulsar. In the 1–15 keV band X-ray pulsars have power-law spectra with energy indices, α , between 0.0 and 1.0 (White, Swank & Holt 1983). The spectra of the non-pulsing sources are softer and have been characterized as either thermal-like with $kT \sim 5$ –10 keV, or power law with $\alpha \sim 2.0$ (e.g. Mason *et al.* 1976; Jones 1977; Parsignault & Grindlay 1978; Mason *et al.* 1980; White & Swank 1982). The latter group is exclusively made up of the low-mass X-ray binaries (LMXRB) which include the bright bulge sources, X-ray burst sources and Sco X-1. The principal properties of the LMXRB and X-ray pulsars are thought to be determined by whether or not the strength of the magnetic field of the neutron star is sufficient to disrupt the inflowing material before it reaches the neutron star surface. This in turn determines whether the emission is from localized hotspots at the magnetic poles, or from the inner region of an accretion disc and a boundary layer between the disc and the neutron-star surface.

The high luminosities of 10^{37} – 10^{38} erg s $^{-1}$ and the detection of X-ray bursts that display blackbody spectra with inferred emission radii of 10 km (Swank *et al.* 1977; Hoffman, Lewin & Doty 1977) convincingly argue that the compact object in most LMXRB is not a white dwarf. The nature of the X-ray continuum emission from LMXRB is currently the subject of much discussion. A thermal bremsstrahlung model only provides an adequate representation of the data if the emitting plasma cloud is Thomson thick (Lamb & Sanford 1979). However, the inferred Thomson depths, τ , of 5 to 15, combined with the observed emission measures give dimensions for the plasma cloud comparable to that of a white dwarf, not of a neutron star. Serlemitsos & Swank (1980, unpublished) have pointed out that a two-component model consisting of a blackbody plus a thermal bremsstrahlung spectrum also gives a good fit to the spectra of several LMXRB; the inferred radius of the blackbody component in this model is typically 10 km. Recently, White, Peacock & Taylor (1985, hereafter WPT) using the *EXOSAT* gas scintillation proportional counter (GSPC) confirmed this result in the case of Sco X-1, but also

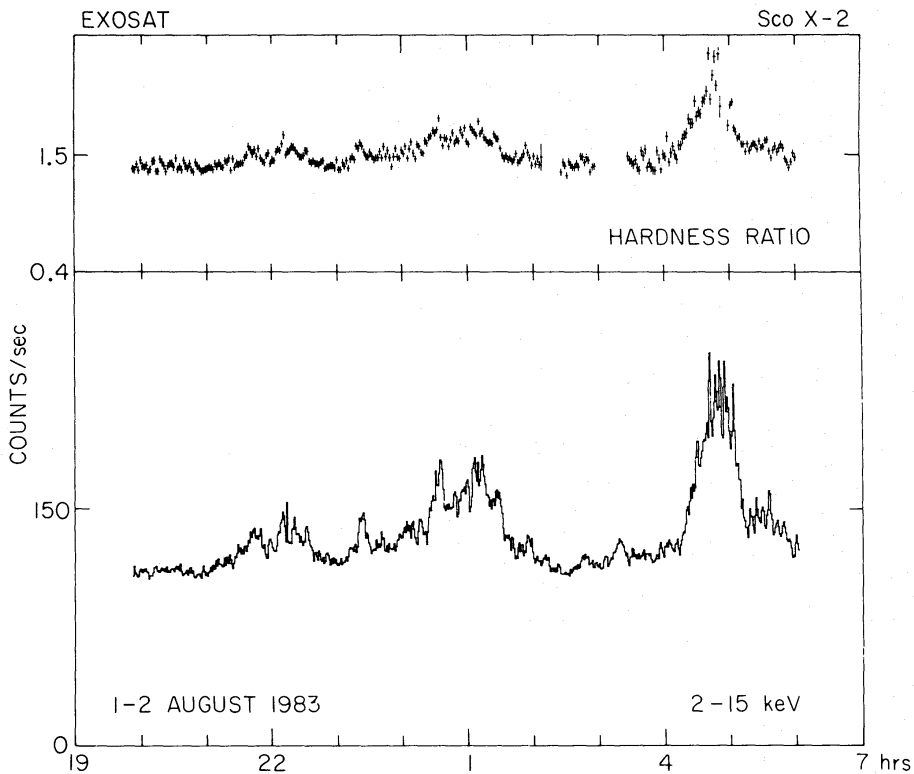


Figure 1. The light curve of Sco X-2. Also given is the hardness ratio obtained by dividing the counts between 7–15 keV by those between 2–7 keV. This source is also sometimes called GX349+2 and X1702–363.

noted that the bremsstrahlung component could be interchanged with the solution to the Kompaneets equation for the Comptonization of low-energy photons on high-energy electrons. In a variant of this model Mitsuda *et al.* (1984), find that GSPC data obtained by the *Tenma* satellite can be fit with a blackbody plus the integrated multi-temperature blackbody spectrum from an optically thick accretion disc.

The energy, width, strength and time variability of the iron *K* line in the X-ray spectra of accreting binaries can provide a useful diagnostic of the geometry of the emission region relative to that of the inflowing material. The search for iron *K* emission from Sco X-1 initially gave conflicting results, with features detected in proportional counter spectra not confirmed by dispersive spectrometers (*cf.* Holt, Boldt & Serlemitsos 1969; Long & Kestenbaum 1978). The gas scintillation detector has an energy resolution that is a factor of 2 better than that of a conventional proportional counter (Peacock *et al.* 1982). The *EXOSAT* GSPC has resolved an iron *K* emission line at 6.7 keV with a full-width-half-maximum, (FWHM), of 0.7 keV in the spectrum of Sco X-1 (WPT). The fact that the line is broad explains why it was not detected in observations using crystal spectrometers. Apart from a few notable exceptions (e.g. Cyg X-3), reports of iron *K* lines from other bright LMXRB based on proportional counter data (e.g. Parsignault & Grindlay 1978) have been inconclusive due to uncertainties in the modelling of the continuum.

In this work the *EXOSAT* GSPC is used to investigate the spectral properties of a sample of six LMXRB. These results are compared with those obtained by WPT from Sco X-1 using the same detector and interpreted in terms of accretion on to a neutron star with a weak magnetic field such that the accretion disc touches the neutron star surface.

2 Results

During the *EXOSAT* verification phase between 1983 June & August, four bright galactic bulge sources, Sco X-2 (X1702–363/GX349+2), X1705–440, GX9+1 (X1758–205) and GX17+2 (X1813–140), and two X-ray burst sources, XB1728–337 and Ser X-1 (XB1837+049), were observed, each for between 6 and 11 hr. Sco X-2 displayed intensity variations of a factor of 2 on a time-scale of minutes; they were correlated with an overall hardening of the spectrum (Fig. 1). Such activity is a characteristic of the Sco X-1 class (Mason *et al.* 1976). The similarity of this light curve to that of Sco X-1 is striking (*cf.* WPT). The other sources were much less active showing at most 10–20 per cent variations. An X-ray burst detected from Ser X-1 was excluded from the analysis.

A background-subtracted 256 pulse height channel spectrum was derived for each observation. The data on Sco X-2 were divided into two according to whether the source count rate was above or below 150 counts s^{−1} and spectra accumulated for each flux state. In the other cases the observed intensity variations were too small to search for associated changes in the spectrum. The following models folded through the detector response were fitted to the spectra:

- (i) PL – Power Law.
- (ii) TB – Thermal Bremsstrahlung.
- (iii) OTTB – Optically thick thermal bremsstrahlung (Chapline & Stevens 1973; Lamb & Sanford 1979).
- (iv) MT+BB – Multi-temperature disc plus blackbody (Mitsuda *et al.* 1984).
- (v) TB+BB – Thermal bremsstrahlung plus blackbody.
- (vi) An unsaturated Comptonized spectrum plus blackbody with the Comptonized spectrum approximated in two ways: (a) UC+BB – function of the form $E^{-\Gamma} \exp(-E/kT_{\text{th}})$ and (b) ST+BB – using a solution to the Kompaneets equation (Sunyaev & Titarchuk 1980).

The fitting procedure included, as a free parameter, absorption in the line-of-sight. In addition, an iron *K* emission line with a Gaussian profile and a fixed FWHM of 0.7 keV (the value found for Sco X-1 by WPT) but variable strength (L_p) and energy was also included. Calibrations on the Crab Nebula indicate that the detector response at a particular energy is known only to 0.5 per cent and this uncertainty was added quadratically to the statistical errors. Fig. 2 summarizes the reduced chi-squared, χ^2_r , for each source and model spectrum. For completeness we also give in Fig. 2 similar results for Sco X-1 at both high and low intensity, taken from WPT. The sampled energy range was chosen to be 2–16 keV for all but Sco X-1, for which it was 2–25 keV (because the detector was operated in a different gain mode).

The models which consistently gave the lowest reduced chi-squared (less than 1.5) were TB+BB, UC+BB and ST+BB. The other two-component model, MT+BB, gave in most cases significantly worse fits; in particular for Sco X-1, where the higher upper energy limit of 25 keV more rigorously constrains the continuum, (a χ^2_r of 2.7 and 5.9 for the two intensity states). The OTTB model also gave unacceptable fits ($\chi^2_r \sim 2$ –7) in all but the case of GX9+1. For the two burst sources Ser X-1 and XB1728–337 a simple bremsstrahlung spectrum gave an acceptable χ^2_r . However, these two objects were a factor of 5 fainter than the other sources and the statistics were

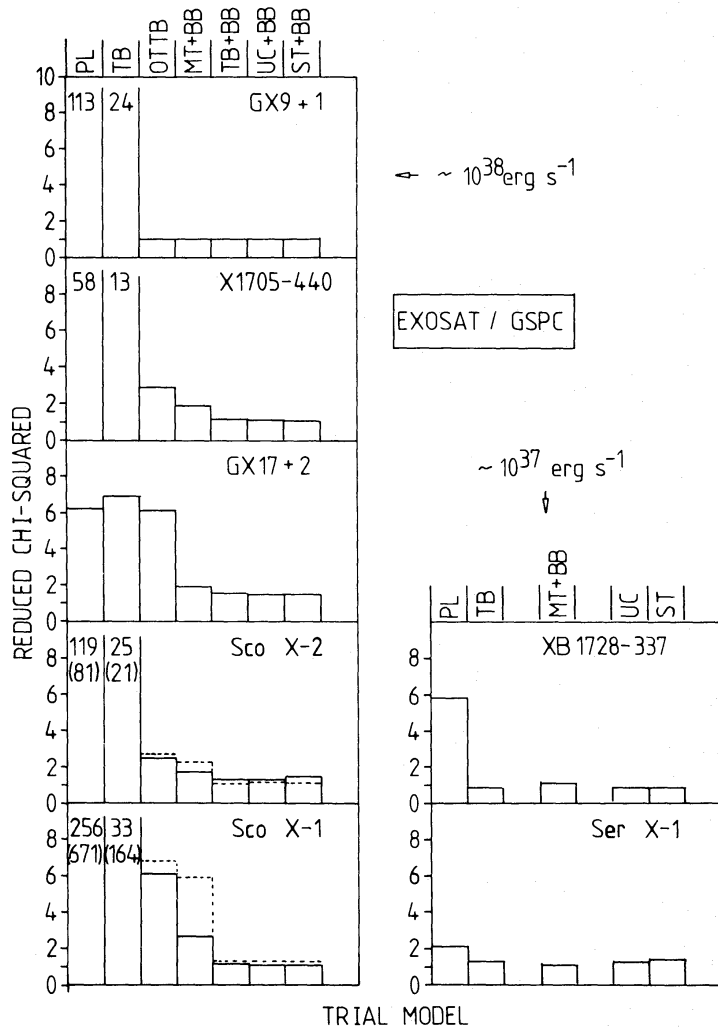


Figure 2. The reduced χ^2 obtained for the various trial models discussed in the text for each of the LMXB in our sample. Also given are the values for Sco X-1 obtained by WPT. The dashed lines represent the fits to the spectra obtained when the source was flaring.

insufficient to rule out more complex models. Had a blackbody component been present with a temperature comparable to that of the other sources, then its luminosity is constrained to <10 per cent (90 per cent confidence) of the total, compared with 10–70 per cent for the others. A power-law model was ruled out in all cases. The MT+BB also gave an acceptable fit, however, given that this is a much more complex model than the UC model there seems little justification in invoking it. The best-fitting parameters for the UC model are given in Table 1a.

The contribution of the blackbody component to the total increased from 40 to 70 per cent between the two intensity states of Sco X-2 while the other component remained constant. In Fig. 3 the two pulse-height spectra taken from the two intensity states are illustrated. The contributions of the blackbody and unsaturated Comptonized components are indicated as histograms. This illustrates that the flaring is caused by increases in the blackbody component. Also given is the incident spectrum after deconvolution from the instrument response.

An iron *K* emission line with a EW ranging between 70 and 130 eV was detected in all the sources except GX9+1 where an upper limit (90 per cent confidence) of 20 eV was set. To investigate the width of the iron line the UC+BB model was re-fitted to the data with the line FWHM as an additional free parameter. The results are summarized in Table 1b with 1σ uncertainties ($\chi^2+2.4$). Fig. 4 illustrates four representative spectra compared to the best-fitting UC+BB model and the residuals from that model. The strength of the iron line in the model has been set to zero to illustrate its significance. The values quoted in Table 1b were obtained using the UC+BB model for the continuum, but do not change significantly when the TB+BB and

Table 1. (a) Continuum parameters.

Source	Γ	kT_{th} (keV)	kT_{bb}^* (keV)	$L_{\text{bb}}/L_{\text{tot}}$ ($10^{38} \text{ erg s}^{-1}$)	L_{tot}^\dagger	R_{bb}^\ddagger (km)
Sco X-1 low	1.2	6	1.5	0.10	0.9	4
high	1.2	6	1.8	0.40	1.4	6
Sco X-2 low	1.6 ± 1.0	6.2 ± 3.0	1.61	0.39	1.7	8
high	1.5 ± 0.4	8.0 ± 3.0	1.63	0.70	2.9	11
GX17+2	0.6 ± 0.5	4.5 ± 1.5	1.04	0.32	1.8	14
X1705–440	0.6 ± 0.2	4.4 ± 0.5	1.32	0.25	1.2	10
GX9+1	0.7 ± 0.4	3.0 ± 0.4	1.97	0.26	1.4	4
Ser X-1	1.5 ± 0.3	6.1 ± 1.0	–	–	0.6	–
XB1728–337	1.2 ± 0.2	7.8 ± 2.1	–	–	0.3	–

(b) Iron *K* line parameters.

Source	L_p ($\text{ph cm}^{-2} \text{ s}^{-1}$)	FWHM (keV)	Energy (keV) ‡	EW (keV)
Sco X-1 low	0.12	0.7	6.7	50
high	0.12	0.7	6.7	25
Sco X-2 low	1.3×10^{-2}	1.1 ± 0.3	6.70 ± 0.05	101 ± 18
high	1.4×10^{-2}	0.8 ± 0.4	6.75 ± 0.05	73 ± 19
GX17+2	1.4×10^{-2}	1.3 ± 0.4	6.55 ± 0.05	108 ± 40
X1705–440	1.0×10^{-2}	1.1 ± 0.3	6.47 ± 0.05	109 ± 22
GX9+1	2.0×10^{-3}	1.0 fixed	–	20
Ser X-1	2.8×10^{-3}	1.0 ± 0.4	6.44 ± 0.10	97 ± 14
XB1728–337	1.8×10^{-3}	1.0 ± 0.4	6.65 ± 0.10	127 ± 35

*Uncertainties are in all cases ± 0.10 keV.

† These assume distances of 9 kpc for the 1 to 20 keV energy band (except for Sco X-1 where 1.5 kpc was used WPT).

‡ In addition systematic uncertainties of 0.05 keV are present.

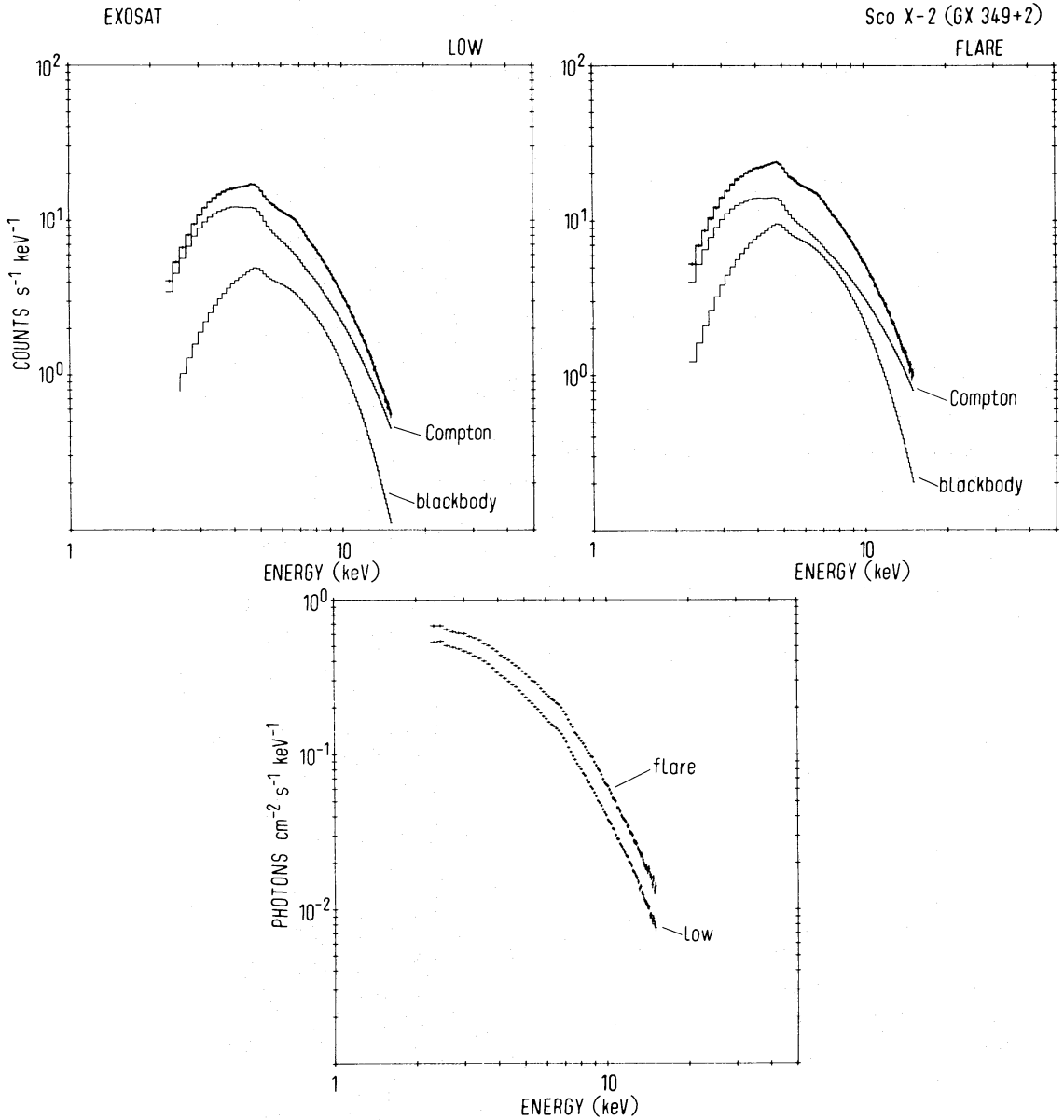


Figure 3. Top: Pulse height spectra obtained from the minimum and maximum intensity levels along with the best-fitting UC+BB model. Also illustrated are the relative contributions of the two components. Bottom: The incident spectra after deconvolution from the detector response.

ST+BB models are used. For the MT+BB model somewhat larger line strengths are obtained if the bandpass of the detector is set to 2–16 keV. However, when the energy range is limited to 5–10 keV this model gives a similar χ^2_r to that obtained from the other two-component models, and identical iron line parameters to those given in Table 1b. The line parameters obtained using the UC+BB, ST+BB and TB+BB continuum models are independent of the energy range selected to fit the continuum. In Fig. 5 the GX9+1 spectral fit is illustrated along with the residuals from that fit. No iron line is included in the fit and the residuals do not indicate any to be present.

The line was resolved in the cases where it was detected to have a typical FWHM of ~ 1 keV. The measured line centroid varied from source to source between 6.44 and 6.75 keV, and the scatter in the derived values is much in excess of the 90 per cent confidence systematic and

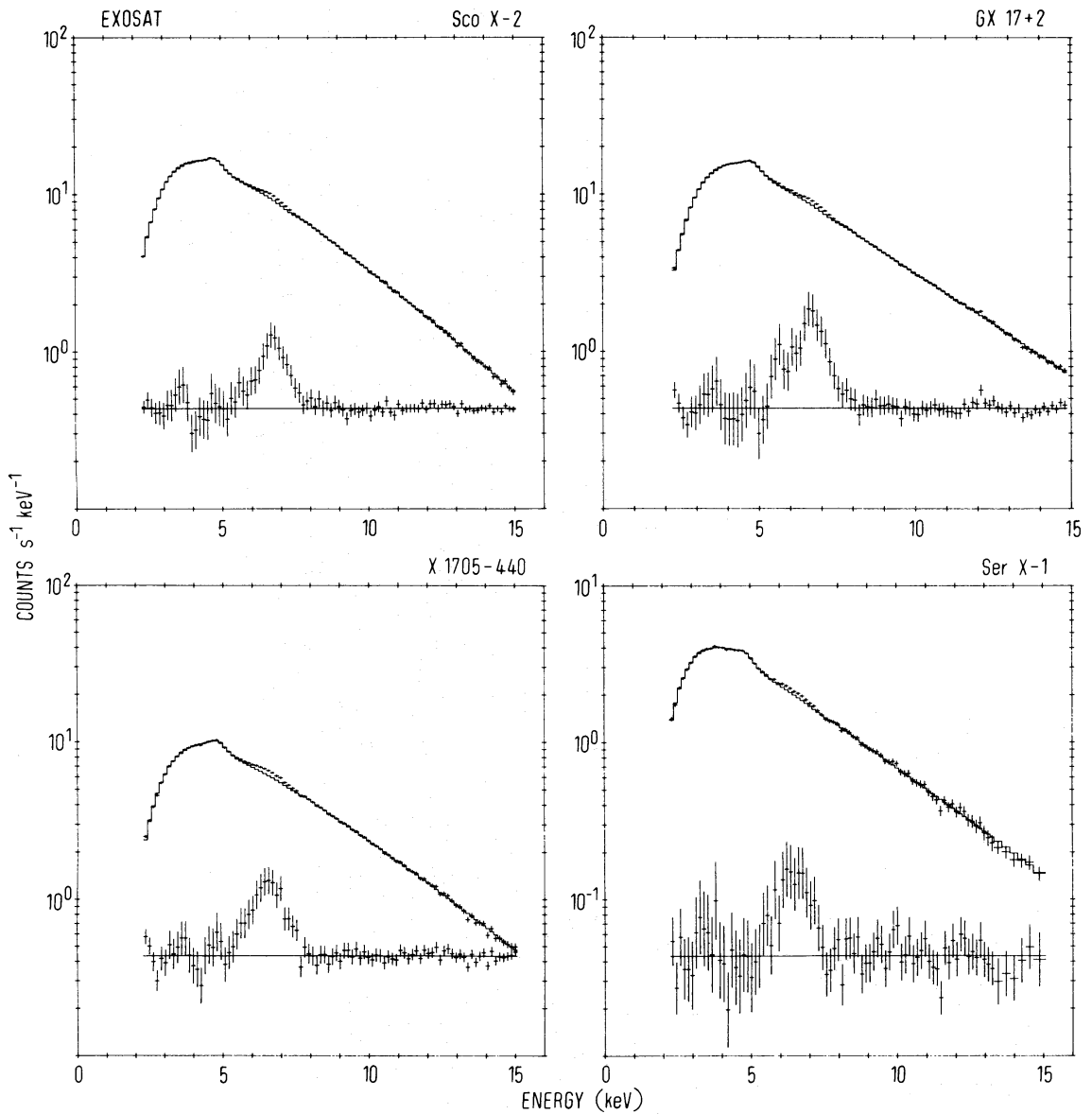


Figure 4. The spectra obtained from the *EXOSAT* GSPC for four of the LMXRB in our sample. The histograms represent the best-fitting spectral model (a blackbody plus an unsaturated Comptonized spectrum). The iron line strength has been set to zero in the model. The residuals from the model are also shown. The broad hump in the spectra at 4.78 keV is an artifact of the detector.

statistical uncertainties of 0.1 keV. For Sco X-2 there does not appear to be any major change in the FWHM, energy or strength of the line when the intensity level changes. Thus the EW of the line decreases during flares.

3 Discussion

The 2–16 keV continuum of the high-luminosity LMXRB can be modelled by a two-component spectrum. This consists of a blackbody plus a component that could be either a thermal bremsstrahlung, or the unsaturated Comptonized spectrum of low-energy photons on high-energy electrons. The flaring activity from Sco X-2 is caused by an increase in the luminosity of the blackbody component, from 40–70 per cent of the total. In the case of Sco X-1 the flares are

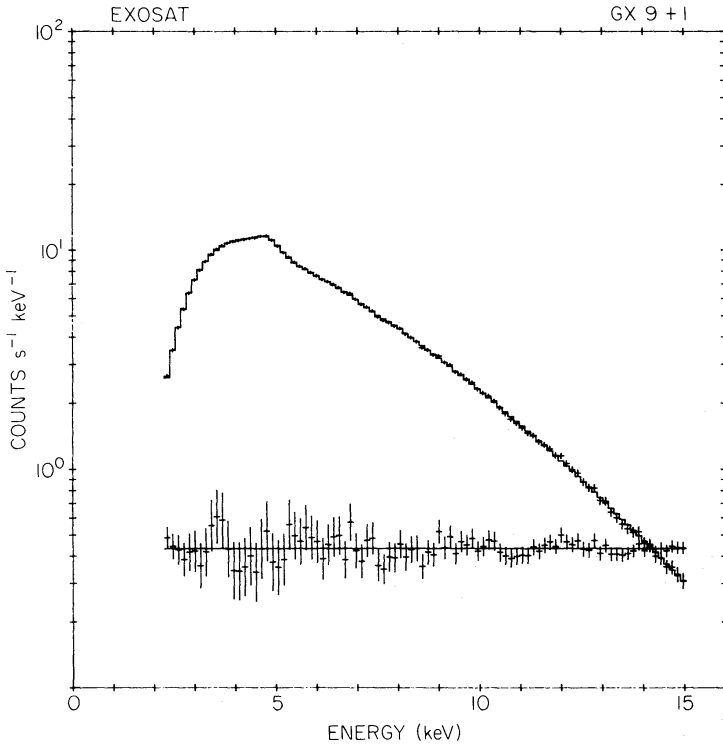


Figure 5. The pulse height spectrum of GX9+1 and the best-fitting UC+BB model along with the residuals from that model. No iron line is included in the modelling. This was the only source in our sample not to show an iron *K* line.

similarly caused by an increase in the blackbody luminosity in that case from 10–40 per cent. The inferred blackbody radius for a spherical emitter ranges from 4 to 14 km, which suggests that it originates from the heated surface of a neutron star at the boundary layer between an accretion disc and the neutron star surface. A thermal bremsstrahlung interpretation for the other component is difficult to understand in the context of disc accretion on to a neutron star since the emission measure of $\sim 10^{60} \text{ cm}^{-3}$ requires, for reasonable optical depths, a radius greater than 10^8 cm . Based on the analogy with Cyg X-1 a Comptonized spectrum seems more likely (WPT). The Sunyaev & Titarchuk (1980) solution to the Kompaneets equation for the upscattering of low-energy photons on a spherical distribution of high-energy electrons gives Thomson depths that range between 11 and 13 with temperatures, kT , of between 2.4 and 3.3 keV; for Cyg X-1 these values are 5 and 27 keV, respectively (Sunyaev & Titarchuk 1980). The alternative suggestion by Mitsuda *et al.* (1984) that one of the two components originate from the integrated multi-temperature spectrum expected from an optically thick accretion disc gives much poorer χ_r^2 and, on this basis alone, is ruled out for Sco X-1 and Sco X-2.

The lower luminosity ($10^{37} \text{ erg s}^{-1}$) burst sources Ser X-1 and XB1728–337 do not require the presence of a blackbody component. This may either be because it is not present, or because the temperature of this component is so low that the bulk of the emission is below the 2 keV threshold of the GSPC. Some burst sources have been reported to show power-law spectra in the 1–15 keV band with $\Gamma \sim 2.0$ (White & Swank 1982 and Mason *et al.* 1980). While neither burst source studied here is well-fitted by a power-law spectrum, we can fit them using a power law that has a high-energy cut-off at $\sim 7 \text{ keV}$ (i.e. the UC model). In several other *EXOSAT* observations of X-ray burst sources using the medium-energy detector (to be reported elsewhere) power-law spectra with high-energy cut-offs $> 20 \text{ keV}$ and blackbody contribution of < 3 per cent are found.

Iron *K* line emission at 6.4–6.7 keV seems to be a common feature of the spectra of LMXRB. Out of a sample of six objects only one, GX9+1, failed to produce a positive detection. The line properties show no obvious correlation with luminosity (Table 1b). The lines detected are broad with atypical FWHM of 0.8–1.3 keV. Comptonization provides the only plausible broadening mechanism (*cf.* WPT). The resulting line centroid and profile then depends on the temperature of the electrons relative to the energy of the injected photons (Pozdnyakov, Sobol & Sunyaev 1979). As found for Sco X-1, by WPT the line FWHM and line centroid energies of 6.6–6.9 keV indicate a Thomson depth of a few and an electron temperature close to 7 keV.

At luminosities of $\sim 10^{37}$ – 10^{38} erg s $^{-1}$, the central X-ray source will evaporate material from the disc surface which will remain in hydrostatic equilibrium to form a hot (10^7 – 10^8 K) accretion disc corona (ADC) with Thomson depths of a few at radii of 10^8 – 10^9 cm (White & Holt 1982; McClintock *et al.* 1982; Fabian, Guilbert & Ross 1982). The recombination of Fe xxvi in the inner ADC seems the most plausible explanation for the line emission (*cf.* Fabian *et al.* 1982). Fluorescence of the outer regions of the disc or the face of the companion star is ruled out since the line would be narrow, centred on 6.4 keV and would only be expected to have an EW of order a few eV (Basko 1978). In the case of Sco X-1 the iron line strength and width remain constant during flares (WPT). This also seems to be the case for Sco X-2 (Table 1b). Since the iron line should respond to any increase in luminosity, this fact suggests that the flaring activity is non-isotropic, i.e. an observer at high inclinations would find the flares to be much smaller.

4 Conclusion

We have found that the spectral properties of a sample of six LMRXB can be qualitatively understood in terms of disc accretion on to a neutron star with a low magnetic field that is less than 10^8 G, such that the accretion disc touches the neutron star surface. In this model the energy release will be approximately equally divided between the inner accretion disc and the neutron star surface (provided the neutron star spins slowly compared to the disc's inner Keplerian period). For the Eddington limited systems a two-component spectrum consisting of a variable blackbody plus a relatively constant unsaturated Comptonized spectrum provides a reasonable description of all the data. The derived blackbody radii are of order 10 km, suggesting it to be associated with the heated surface of a neutron star. The other component may come from the inner disc region. The blackbody component does not appear to be present at the same level in the lower luminosity systems ($\sim 10^{37}$ erg s $^{-1}$). This may suggest that the neutron star has in these systems been spun up to equilibrium with the inner Keplerian period of the accretion disc (~ 1 ms) such that little energy is given up in the boundary layer.

Note: When this paper was close to completion, van der Klis *et al.* (1985) reported the discovery of quasi-periodic oscillations with a period of 25–50 ms from the bright LMXB GX5–1. The subsequent discovery of similar oscillations from Sco X-1 and Cyg X-2 suggests that this phenomenon may be relatively common amongst the LMXRB (Middleditch & Priedhorsky 1985; Hasinger *et al.* 1985). These oscillations may be related to those seen from dwarf novae in outburst (*cf.* Cordova *et al.* 1980). It has been suggested that the oscillations in LMXB may be caused by the beat between the underlying rotation of a neutron star and the Keplerian period at a magnetospheric boundary (Alpar & Shaham 1985). The qualitative picture outlined above can only be consistent with the presence of a magnetosphere if its radius is less than about a stellar radius above the neutron star surface. Any substantial magnetosphere greater than this would disrupt the inner disc such that the bulk of the gravitational energy will be released at the neutron star surface (*cf.* Lewin & van Paradijs 1985). If this is the case then the spectrum should

be dominated by blackbody emission from the neutron star surface (*cf.* Alme & Wilson 1974), unless the inner radiation pressure region of the disc is sufficiently bloated to obstruct the line-of-sight to the central source. Another possibility is that the oscillations are generated in the boundary layer (*cf.* King 1985).

Acknowledgments

We thank all those involved with the development of the GSPC. Walter Lewin made some useful comments on an earlier manuscript. The *EXOSAT* Observatory Team are thanked for their support.

References

- Alme, M. L. & Wilson, J. R., 1974. *Astrophys. J.*, **194**, 147.
 Alpar, M. A. & Shaham, J., 1985. *Nature*, **316**, 239.
 Basko, M. M., 1978. *Astrophys. J.*, **223**, 268.
 Chapline, H., Jr & Stevens, J., 1973. *Astrophys. J.*, **184**, 1041.
 Cordova, F. A., Chester, T. J., Tuohy, I. R. & Garmire, G. P., 1980. *Astrophys. J.*, **235**, 163.
 Fabian, A. C., Guilbert, P. W. & Ross, R. R., 1982. *Mon. Not. R. astr. Soc.*, **199**, 1045.
 Hasinger, G., Langmeier, A., Sztajno, M. & White, N. E., 1985. *IAU Circ. No.* 4070.
 Hoffman, J. A., Lewin, W. H. G. & Doty, J., 1977. *Mon. Not. R. astr. Soc.*, **179**, 57p.
 Holt, S. S., Boldt, E. A. & Serlemitsos, P. J., 1969. *Astrophys. J.*, **158**, L155.
 Jones, C., 1977. *Astrophys. J.*, **214**, 856.
 King, A. R., 1985. *Nature*, **313**, 291.
 Lamb, P. & Sanford, P. W., 1979. *Mon. Not. R. astr. Soc.*, **188**, 555.
 Lewin, W. H. G. & van Paradijs, J., 1985. *Astr. Astrophys.*, in press.
 Long, K. S. & Kestenbaum, H. L., 1978. *Astrophys. J.*, **226**, 276.
 Mason, K. O., Charles, P. A., White, N. E., Culhane, J. L., Sanford, P. W. & Strong, K. T., 1976. *Mon. Not. R. astr. Soc.*, **177**, 513.
 Mason, K. O., Middleditch, J., Nelson, J. E. & White, N. E., 1980. *Nature*, **287**, 516.
 McClintock, J. E., London, R. A., Bond, H. E. & Graver, A. O., 1982. *Astrophys. J.*, **258**, 245.
 Middleditch, J. & Priedhorsky, W., 1985. *IAU Circ. No.* 4060.
 Mitsuda, K. *et al.*, 1984. *Publs astr. Soc. Pacif.*, **36**, 741.
 Parsignault, D. & Grindlay, J. E., 1978. *Astrophys. J.*, **225**, 970.
 Peacock, A., Andersen, R. D., Manzo, G., Taylor, B. G., Villa, G., Re, S., Ives, J. C. & Kellock, S., 1982. Proceedings of the XV ESLAB Symposium, p. 525, ed. Andresen, R. D., Reidel, Dordrecht, Holland.
 Pozdnyakov, L. A., Sobol, I. M. & Sunyaev, R. A., 1979. *Astr. Astrophys.*, **75**, 214 (PSS).
 Swank, J. H., Becker, R. H., Boldt, E. A., Holt, S. S., Pravdo, S. H. & Serlemitsos, P. J., 1977. *Astrophys. J.*, **212**, L73.
 Sunyaev, R. A. & Titarchuk, L. G., 1980. *Astr. Astrophys.*, **86**, 121.
 van der Klis, M., Jansen, F., van Paradijs, J., Lewin, W. H. G., van den Heuvel, J., Trümper, J. E. & Sztajno, M., 1985. *Nature*, **316**, 225.
 White, N. E. & Holt, S. S., 1982. *Astrophys. J.*, **257**, 318.
 White, N. E., Peacock, A. & Taylor, B. G., 1985. *Astrophys. J.*, in press (WPT).
 White, N. E. & Swank, J. H., 1982. *Astrophys. J.*, **253**, L61.
 White, N. E., Swank, J. H. & Holt, S. S., 1983. *Astrophys. J.*, **270**, 711.